Supporting Information

Realizing Highly Efficient Deep-Blue Organic Light-Emitting Diodes towards Rec.2020 Chromaticity by Restricting the Vibration of the Molecular Framework

Chuan Li [a], Kai Zhang [b], Yanju Luo [c], Yang Yang [a], Yong Huang [a], Mengjiao Jia [a], Yuling He [a], Yue Lei [a], Jianxin Tang [b*], Yan Huang [a], and Zhiyun Lu [a*]

DOI: XXXXXXXXXXXXX

SUPPORTING INFORMATION

Table of Contents

1. Experimental procedures

1.1 General information

Materials. Unless stated otherwise, all reagents and anhydrous solvents were purchased from *Bidepharm Ltd. Co.*, *Energy Chemical Co.* or *J&K scientific Ltd. Co.* and used without further purification. All solvents used in photophysical measurements were of analytical grade and freshly distilled before use. The target compounds BOC-PC and BOC-PSi was purified through recrystallization followed by vacuum sublimation. The DPEPO host materials was purchased from Luminescence Technology Corporation and used as received without further purification.

Methods. ^{1}H NMR and ^{13}C NMR spectra were acquired on a Bruker AVANCE II-400 MHz spectrometer at 400 and 100 MHz in $CDCl_3$, respectively. Tetramethylsilane (TMS) was utilized as an internal standard. All chemical shift data were recorded in the standard δ notation of parts per million (ppm). The splitting patterns observed were reported as s (singlet), d (doublet), t (triplet), and m (multiplet). High-resolution MS spectra were obtained via a QTOF Premier ESI mass spectrometer (Micromass, Manchester, UK). UV-visible spectra were recorded using a HITACHI U-2910 spectrophotometer. Steady-state photoluminescence (PL) at room temperature (RT) and phosphorescence measurements at 77 K were conducted on a Horiba Jobin Yvon FluoroMax fluorescence spectrophotometer. PL quantum efficiency were measured on a Hamamatsu UV-NIR (C13534) absolute PL quantum yield spectrometer. Transient PL decay profiles at room temperature (from 77 K to 295 K) under a nitrogen (vacuum) atmosphere were measured using a Horiba Jobin Yvon FluoroHub-B with a single-photon counting controller. Single-crystal X-ray diffraction data was collected from a Bruker D8 Venture X-ray single-crystal diffractometer with a graphite monochromator and Cu-Kα radiation. Single crystal of two compounds were obtained by slowly evaporating a saturated solution of mixed solvents (dichloromethane and ethanol) at room temperature. Cyclic voltammetry measurements were conducted on a LANLIKE LK2010 electrochemical analyzer employing a three-electrode system. A glassy carbon electrode was used as the working electrode, while a platinum wire was used as the auxiliary electrode and an Ag/Ag^{+} electrode served as the pseudo-reference electrode. Fc/Fc+ was used as an internal standard for calibration purposes. The crystallographic data of BOC-PC and BOC-PSi has been deposited with a CCDC number of 2307420 and 2307421 in the Cambridge Structural Database.

Computational method. The geometry of the ground state (S_0) was optimized using the density functional theory (DFT) method with a PBE0 functional and 6-31G** basis. The energy and optimized configuration of excited states were calculated based on PBE0/6-31G**. Vibration analysis was then carried out on the optimized geometries of the S_0 and S_1 states, also based on PBE0/6-31G**. The calculations described above were carried out using the polarizable continuum model (toluene) within the

Gaussian 16 software package. To calculate the reorganization energy, the Dushin program was utilized.[1] The associated Huang-Rhys factor was calculated with $S_i=\lambda_i/(h\cdot v_i)$ formular. Here, the symbol λ_i represents the decomposed reorganization energy, v_i denotes the frequency of normal vibration mode, h represents Planck constant.

1.2 Synthesis

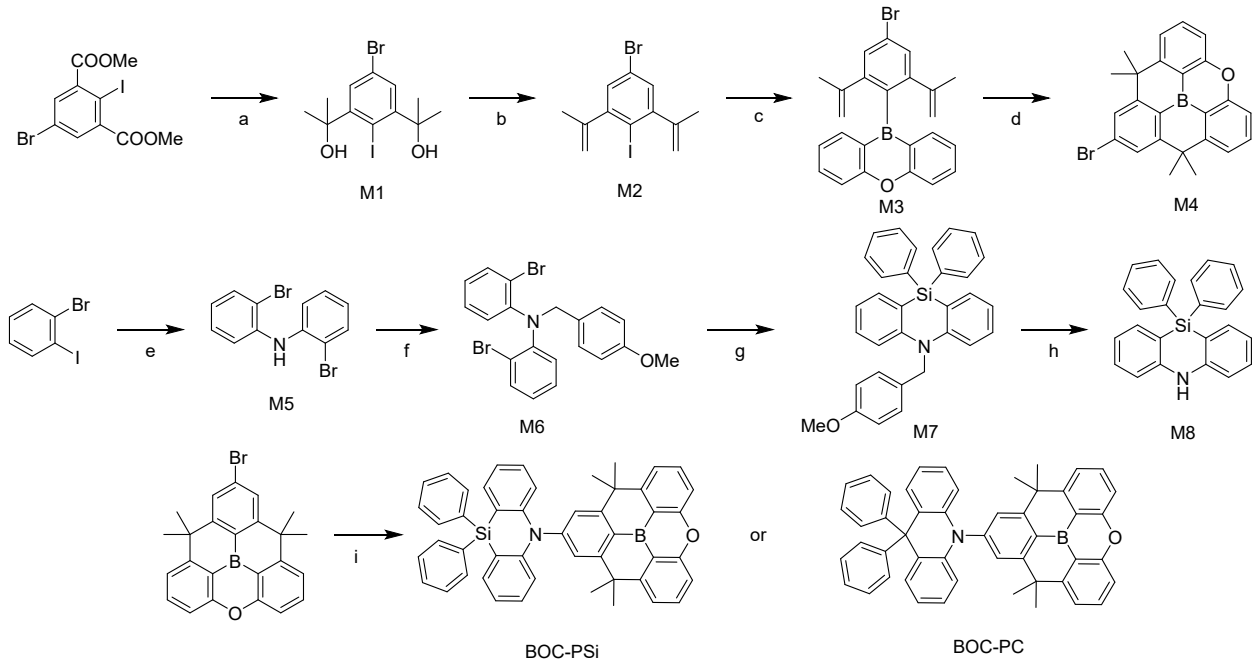

Condition: a) CH_3MgI, I_2, Et_2O, reflux. b) TsOH, toluene, reflux. c) *n*-BuLi, Et_2O, 10-bromo-10*H*-dibenzo[*b*,*e*][1,4]oxaborinine. d) $Sc(CF_3SO_3)_3$, DCE, reflux. e) $Pd(OAc)_2$, 1-bromo-2-iodobenzene, bis[2-(diphenylphosphino)phenyl] ether, *t*-BuONa, reflux. f) NaH, 4-methoxybenzyl bromide, DMF, RT. g) *n*-BuLi, dichlorodiphenylsilane, RT. h) DDQ, toluene/H_2O, reflux. i) $Pd_2(dba)_3$, diphenylacridine/ phenazasiline, $(t\text{-Bu})_3PHBF_4$, *t*-BuONa.

Scheme S1. The synthetical routs of donor, acceptor and target compounds BOC-PC and BOC-PSi.

Synthesis of 1,1'-(5-bromo-2-iodo-1,3-phenylene)bis(ethan-1-ol) (M1)

The synthesis conditions of intermediate M1 are slightly different from those in the literature.[2] To a solution of methyl 3-acetoxy-5-bromo-2-iodobenzoate (20 g, 50.1 mmol) in toluene (150 mL), a Grignard reagent was slowly added. The Grignard reagent was freshly prepared by mixing CH_3I (14 mL, 226.7 mmol) and Mg (6 g, 250 mmol) in ether (100 mL). The resulting mixture was refluxed with continuous stirring for 2 hours. After that, I_2 (10 g, 40 mmol) in THF (60 mL) was slowly added. The reaction mixture was stirred at room temperature for 1 hours. The reaction was quenched by adding saturated aqueous solutions of Na_2SO_3. The mixture was separated by filtration and then the organic layer was extracted with dichloromethane three times. Subsequently, the organic extracts were washed using a saturated

aqueous solution of $NaHCO_3$ and brine, then dried with $MgSO_4$ and evaporated under reduced pressure. The mixture was purified using column chromatography on silica gel with EA/PE = 1/4 as the eluent, resulting in the crude 7.1 g product (17.8 mmol) of M1 as a faint yellow solid in a 36% yield. ^{1}H NMR (400 MHz, $CDCl_3$) δ (ppm): 7.71 (s, 2H, ArH),1.84 (s, 12H, CH_3).

Synthesis of 5-bromo-2-iodo-1,3-di(prop-1-en-2-yl)benzene (M2)

In a reaction vessel, a solution of M1 (7.1 g, 17.80 mmol) and *p*-toluenesulfonic acid monohydrate (0.688 g, 3.6 mmol) in toluene (50 mL) was heated under reflux in air for 1 hour. After cooling to room temperature, the reaction mixture was neutralized by addition of a saturated aqueous solution of $NaHCO_3$. Then the organic layer was extracted with DCM three times. The organic extracts were washed with brine and dried with $MgSO_4$. After filtration, and volatiles were evaporated under reduced pressure. The crude product was further purified using column chromatography on silica gel with PE as the eluent. This step yielded 6.13 g (16.91 mmol) of M2 in a 97% yield as a white solid. ^{1}H NMR (400 MHz, $CDCl_3$) δ (ppm): 7.18 (s, 2H, ArH), 5.22 (s, 2H, CH), 4.90 (s, 2H, CH), 2.06 (s, 6H, CH_3).

Synthesis of 10-(4-bromo-2,6-di(prop-1-en-2-yl)phenyl)-10*H*-dibenzo[*b*,*e*][1,4]oxaborinine (M3)

At −78 °C, a solution of *n*-BuLi in hexane (1.6 M, 1.9 mL, 3.04 mmol) was added dropwise to a solution of M2 (1 g, 2.76 mmol) in dry ether (50 mL). The resulting mixture was stirred at this temperature for 1 h. A solution of 9-bromo-9,10-dihydro-9-boraanthracene (Prepared from bis[2-(trimethylsilanyl)-phenyl] ether (800 mg, 3.09 mmol) and BBr_3 (3.5 mmol) according to the reference,[3] the difference is that the reaction solvent and remaining BBr_3 are directly removed by a vacuum oil pump equipped with cold hydrazine, and then the resulted yellow compound is dissolved in dry ether for the next reaction step) in dry (20 mL) was then added dropwise to the reaction mixture at −78 °C. After the addition is completed, the reaction mixture was allowed to slowly rise to room temperature and stirred overnight. The reaction was quenched with a saturated aqueous solution of $NaHCO_3$ and extracted with DCM three times. The organic extracts were washed with brine and dried with $MgSO_4$. After filtration, volatiles were removed under reduced pressure. The crude product was further purified by column chromatography on silica gel using a 10/1 PE/DCM mixture as the eluent. This step gives 315 mg of product as white solid with yield of 28%. ^{1}H NMR (400 MHz, $CDCl_3$) δ (ppm): 7.69-7.64 (m, 4H, ArH), 7.50 (d, J = 8.4 Hz, 2H, ArH) 7.46 (s, 2H, ArH) 7.19 (t, J_1 = 14.8 Hz, J_2 = 7.2 Hz, 2H, ArH) 4.64 (s, 2H, CH) 4.46 (s, 2H, CH) 1.87 (s, 6H, CH_3).

Synthesis of 10-bromo-8,8,12,12-tetramethyl-8,12-dihydro-4-oxa-3a2-boradibenzo[*cd*,*mn*]pyrene (M4)

A solution of M3 (1.6 g, 3.85 mmol) and $Sc(OTf)_3$ (1.89 g, 3.85 mmol) in 1,2-dichloroethane (800 mL) was refluxed with stirring for 4 days. After cooling the reaction mixture to room temperature, a saturated

aqueous solution of $NaHCO_3$ was added. The organic layer was extracted three times with dichloromethane, and the organic extracts dried with $MgSO_4$. After filtration, the volatiles were evaporated under reduced pressure. The crude product was purified using column chromatography on silica gel with PE as the eluent, giving 800 mg (1.93 mmol) of M4 as a white solid in 50% yield. ^{1}H NMR (400 MHz, $CDCl_3$) δ (ppm): 7.81-7.77 (m, 4H, ArH), 7.51 (d, J = 7.6 Hz, 2H, ArH) 7.40 (d, J = 8.4 Hz, 2H, ArH) 1.78 (s, 12H, CH_3).

Synthesis of bis(2-bromophenyl)amine (M5)

The reaction conditions used in this procedure are slightly different from those reported in the literature.[4] In a nitrogen atmosphere, 1-bromo-2-iodobenzene (45 g, 160.00 mmol), 2-bromoaniline (20 g, 175.47 mmol), sodium *tert*-butoxide (21 g, 218.50 mmol), Palladium acetate (175 mg, 0.78 mmol), and bis[2-(diphenylphosphino)phenyl] ether (640 mg, 1.19 mmol) were dissolved in toluene (200 mL) and refluxed for 12 hours. The resulting mixture was then cooled to room temperature, and the solvent was evaporated before diluting the residue with water and extracting it with dichloromethane. The organic volatiles were removed under reduced pressure to yield the crude product, which was subsequently purified by column chromatography to obtain the 50.5 g product as a white solid. Yielded 97%. ^{1}H NMR (400 MHz, DMSO-d_6) δ (ppm): 7.64 (dd, J_1 = 9.6 Hz, J_2 = 1.6 Hz, 2H, ArH), 7.30 (t, J_1 = 15.6 Hz, J_2 = 8.4 Hz, 2H, ArH) 7.06-7.02 (m, 3H, ArH) 6.93 (t, J_1 = 15.2 Hz, J_2 = 8.0 Hz, 2H, ArH).

Synthesis of 2-bromo-*N*-(2-bromophenyl)-*N*-(4-methoxybenzyl)aniline (M6)

To a stirring solution of sodium hydride (60% dispersed in mineral oil, 3.6 g, 88.89 mmol) in 65 mL dimethylformamide (DMF), M5 (10 g, 30.86 mmol) was added slowly and stirred for 1 hour before adding 1-(chloromethyl)-4-methoxybenzene (10 g, 64.82 mmol). The reaction mixture was stirred for an additional 14 hours and then poured into 500 mL ice water. The crude product was collected and washed with water, followed by purification through column chromatography on silica gel with a DCM/PE = 1/5 eluent. This step gives the 11.88 g white powder product with yield of 87%. ^{1}H NMR (400 MHz, $CDCl_3$) δ (ppm): 7.59 (dd, J_1 = 8.0 Hz, J_2 = 1.6 Hz, 2H, ArH), 7.45 (d, J = 8.8 Hz, 2H, ArH) 7.18 (t, J_1 = 15.2 Hz, J_2 = 7.2 Hz, 2H, ArH) 6.98-6.91 (m, 4H, ArH) 6.82 (d, J = 8.4 Hz, 2H, ArH) 4.79 (s, 2H, CH_2) 3.77 (s, 3H, CH_3).

Synthesis of 5-(4-methoxybenzyl)-10,10-diphenyl-5,10-dihydrodibenzo[*b*,*e*][1,4]azasiline (M7)

In a nitrogen-filled environment, M6 (9 g, 20.1 mmol) was dissolved in anhydrous ether (60 mL) and cooled to 0°C. *n*-BuLi (1.6 M, 28 mL, 44.80 mmol) was added dropwise and stirred for 1 hour before slowly injecting dichlorodiphenylsilane (5.6 g, 22.1 mmol) with stirring. The reaction solution was warmed to room temperature and stirred overnight. Upon pouring the reaction mixture into 50 mL water, then the resulted mixture was separated by filtration. Finally, column chromatography on silica gel using

a DCM/PE = 1/5 was performed to purify the crude product and obtain the 8.0 g white powder product. Yield: 85%. ^{1}H NMR (400 MHz, $CDCl_3$) δ (ppm): 7.60 (dd, J_1 = 7.6 Hz, J_2 = 1.6 Hz, 4H, ArH), 7.55 (dd, J_1 = 7.2 Hz, J_2 = 1.6 Hz, 2H, ArH) 7.46-7.36 (m, 6H, ArH) 7.31 (td, J_1 = 17.6 Hz, J_2 = 8.8 Hz J_3 = 1.6 Hz, 2H, ArH) 7.13 (d, J = 8.8 Hz, 2H, ArH) 7.05-6.99 (m, 4H, ArH) 6.85 (d, J = 8.8 Hz, 2H, ArH) 5.19 (s, 2H, CH_2) 3.81 (s, 3H, CH_3).

Synthesis of 10,10-diphenyl-5,10-dihydrodibenzo[*b*,*e*][1,4]azasiline (M8)

The mixture of M7 (6.8 g, 14.50 mmol), 2,3-dichloro-5,6-dicyano-1,4-benzoquinone (DDQ, 5.46 g, 37.54 mmol), toluene (68 mL), and H_2O (6.8 mL) was refluxed at 100 °C for 14 hours. The mixture was then cooled to room temperature and extracted with ethyl acetate. The organic layer was concentrated by evaporating solvents. The crude product was purified by column chromatography on silica gel using a DCM/PE (1/3, v/v) solvent system, resulted in a 1.36 g white powder with yield of 27%. ^{1}H NMR (400 MHz, actone-d_6) δ (ppm): 7.59 (dd, J_1 = 7.6 Hz, J_2 = 1.6 Hz, 4H, ArH), 7.55 (d, J = 7.2 Hz, 2H, ArH) 7.43-7.33 (m, 8H, ArH) 7.10 (d, J = 8.4 Hz, 2H, ArH) 6.93 (t, J_1 = 15.2 Hz, J_2 = 8.0 Hz, 2H, ArH).

Synthesis of 9,9-diphenyl-10-(8,8,12,12-tetramethyl-8,12-dihydro-4-oxa-3a^2-boradibenzo[*cd*,*mn*]pyren-10-yl)-9,10-dihydroacridine (BOC-PC)

300 mg (0.73 mmol) of M4, 300 mg (0.90 mmol) diphenylacridine, 66 mg (0.072 mmol) of Tris(dibenzylideneacetone)dipalladium, 84 mg (0.290 mmol) of tri-*tert*-butylphosphine tetrafluoroborate, 120 mg (1.25 mmol) of sodium *tert*-butoxide and 15 mL dry toluene were added into a flask. The mixture was bubbled with nitrogen for 30 minutes to remove oxygen and then refluxed under N_2 atmosphere at 110°C for 48 hours. After cooling to room temperature, insoluble compounds were filtered under reduced pressure and the residue was washed with DCM. The organic solvent was evaporated and the crude compound was purified via column chromatography with PE: DCM = 5/1 as solvent system, resulting in 260 mg of white powder product with yield of 54%. ^{1}H NMR (400 MHz, $CDCl_3$) δ (ppm): 7.79 (t, J_1 = 16.0 Hz, J_2 = 8.0 Hz, 2H, ArH), 7.51 (d, J = 7.6 Hz, 2H, ArH), 7.41 (d, J = 8.0 Hz, 2H, ArH), 7.34-7.28 (m, 6H, ArH), 7.25 (s, 2H, ArH), 7.09-7.05 (m, 6H, ArH), 6.96-6.88 (m, 4H, ArH), 6.55 (d, J = 8.8 Hz, 2H, ArH), 1.71 (s, 12H, CH_3). ^{13}C NMR (100 MHz, $CDCl_3$) δ (ppm): 158.9, 158.1, 155.8, 146.6, 142.4, 134.5, 130.6, 130.0, 129.9, 127.7, 127.0, 126.8, 126.3, 120.2, 114.3, 113.6, 56.9, 43.5, 33.9. HRMS (ESI): calcd.: 668.3125 $[M + H]^+$; found: 668.3126.

Synthesis of 10,10-diphenyl-5-(8,8,12,12-tetramethyl-8,12-dihydro-4-oxa-3a^2-boradibenzo[*cd*,*mn*]pyren-10-yl)-5,10-dihydrodibenzo[*b*,*e*][1,4]azasiline (BOC-PSi)

In a flask, 300 mg (0.72 mmol) of M4 and 342 mg (0.98 mmol) of M8 were added along with 66 mg (0.072 mmol) of Tris(dibenzylideneacetone)dipalladium, 84 mg (0.290 mmol) of tri-*tert*-butylphosphine tetrafluoroborate, 120 mg (1.25 mmol) of sodium *tert*-butoxide, and 15 mL of dry toluene. The mixture

was bubbled with nitrogen for 30 minutes to remove oxygen and then refluxed under a N_2 atmosphere at 110°C for 48 hours. After cooling to room temperature, insoluble compounds were filtered under reduced pressure, the residue was washed with DCM, and the organic solvent was evaporated. The crude compound was purified via column chromatography with PE/DCM = 5/1 as eluent and recrystallization, giving 230 mg of white powder product with yield of 47%. ^{1}H NMR (400 MHz, $CDCl_3$) δ (ppm): 7.81 (t, J_1 = 16.0 Hz, J_2 = 8.0 Hz, 4H, ArH), 7.69 (dd, J_1 = 7.6 Hz, J_2 = 2.0 Hz, 4H, ArH), 7.65 (dd, J_1 = 7.2 Hz, J_2 = 1.6 Hz, 2H, ArH), 7.54-7.53 (m, 4H, ArH), 7.44-7.39 (m, 8H, ArH), 7.17 (t, J_1 = 17.6 Hz, J_2 = 8.8 Hz, 2H, ArH), 6.95 (t, J_1 = 14.4 Hz, J_2 = 7.2 Hz, 2H, ArH), 6.58 (d, J = 8.8 Hz, 2H, ArH), 1.78 (s, 12H, CH_3). ^{13}C NMR (100 MHz, $CDCl_3$) δ (ppm): 158.9, 155.9, 150.0, 147.8, 136.1, 136.0, 135.7, 134.6, 130.5, 129.6, 127.9, 126.9, 120.2, 119.8, 117.1, 115.3, 113.6, 43.6, 34.0. HRMS (ESI): calcd.: 684.2894 [M + H]; found: 684.2878.

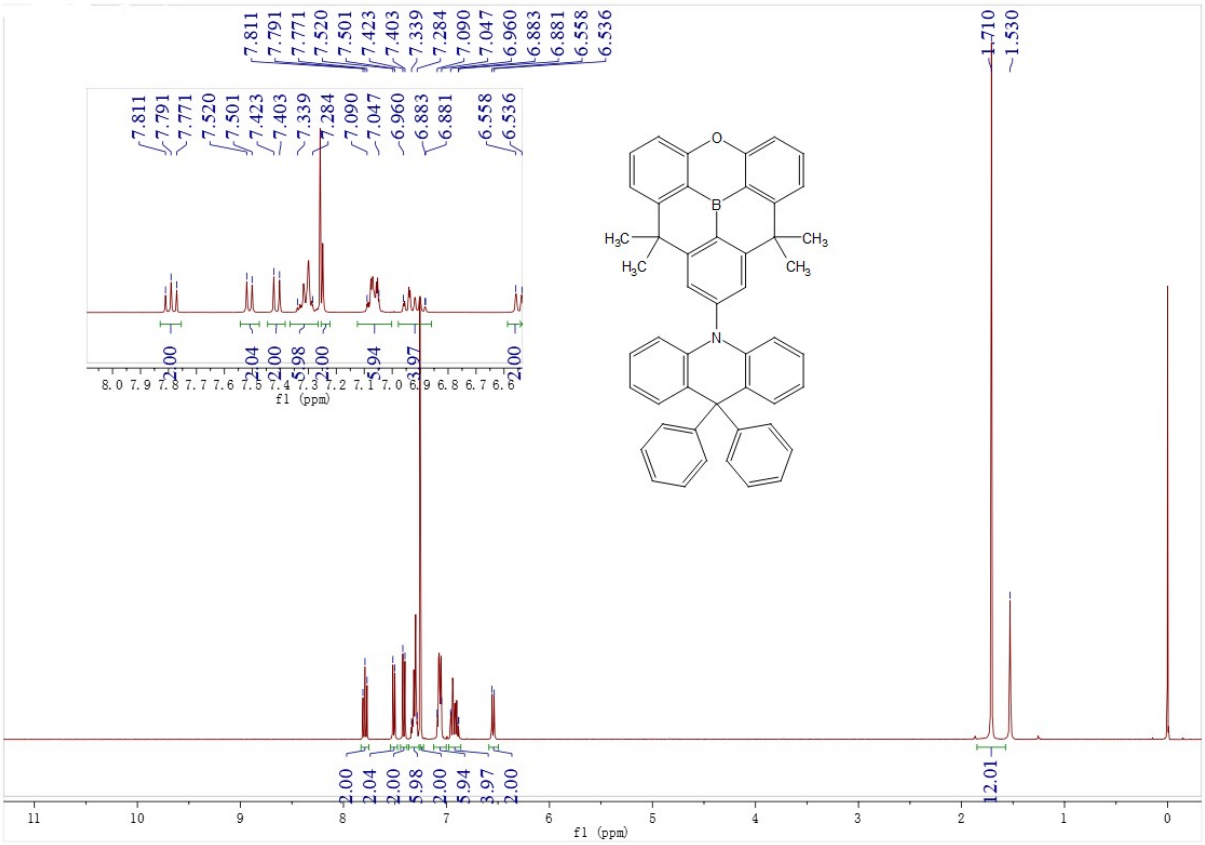

Figure S1. The ^{1}H NMR spectrum of BOC-PC in $CDCl_3$.

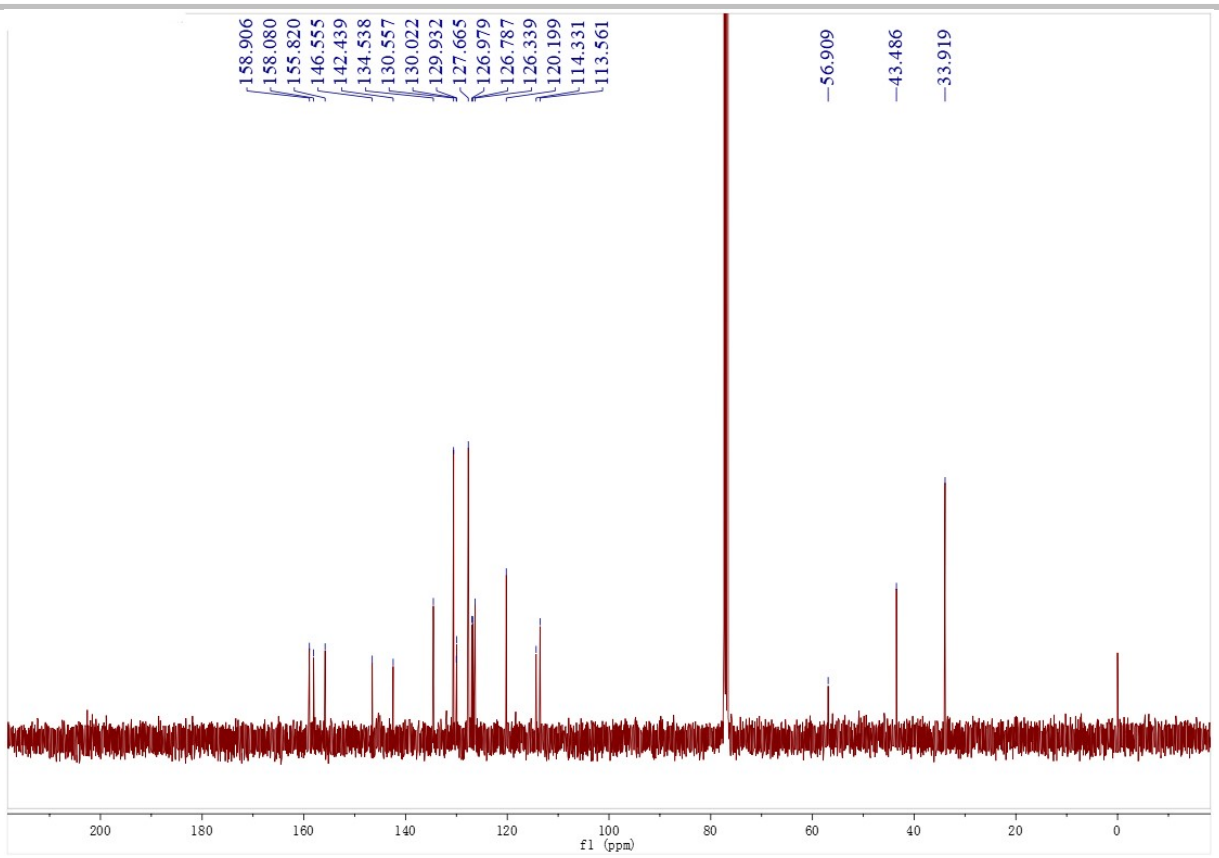

Figure S2. The ^{13}C NMR spectrum of BOC-PC in $CDCl_3$.

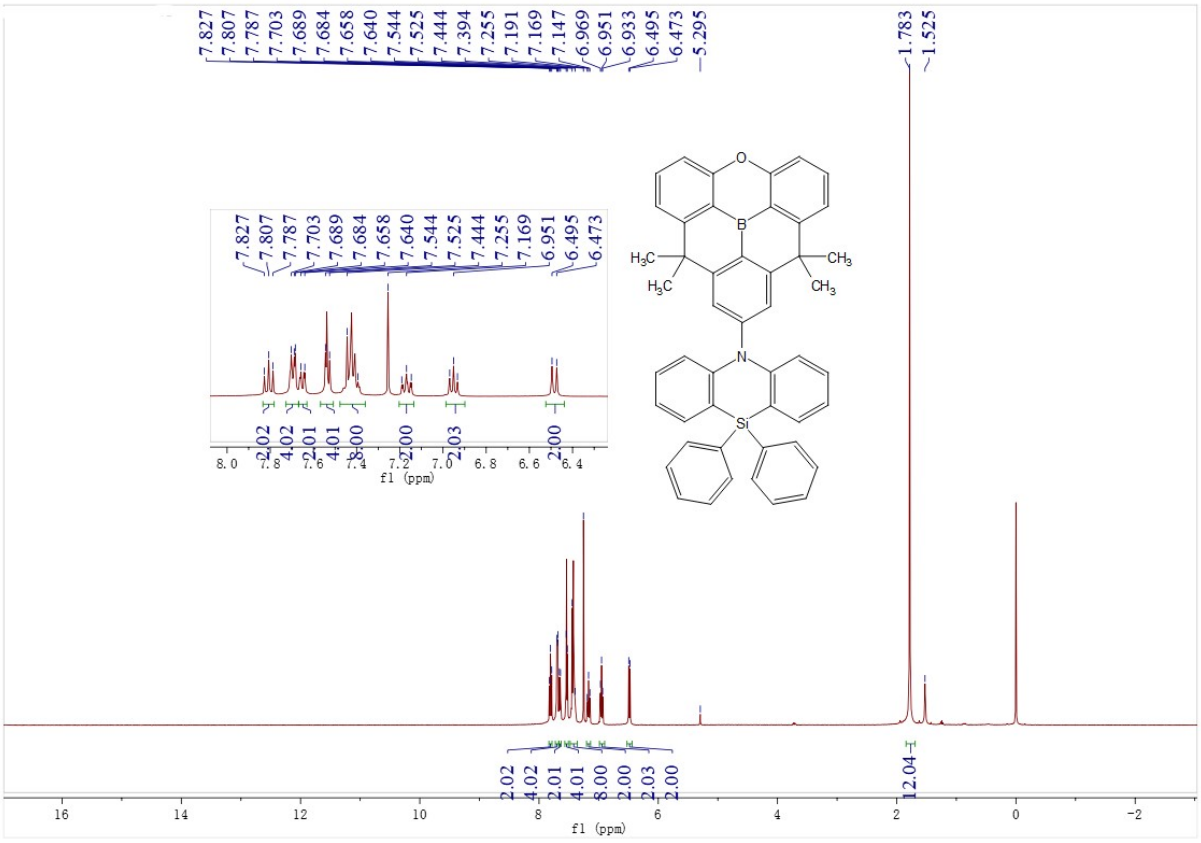

Figure S3. The ^{1}H NMR spectrum of BOC-PSi in $CDCl_3$.

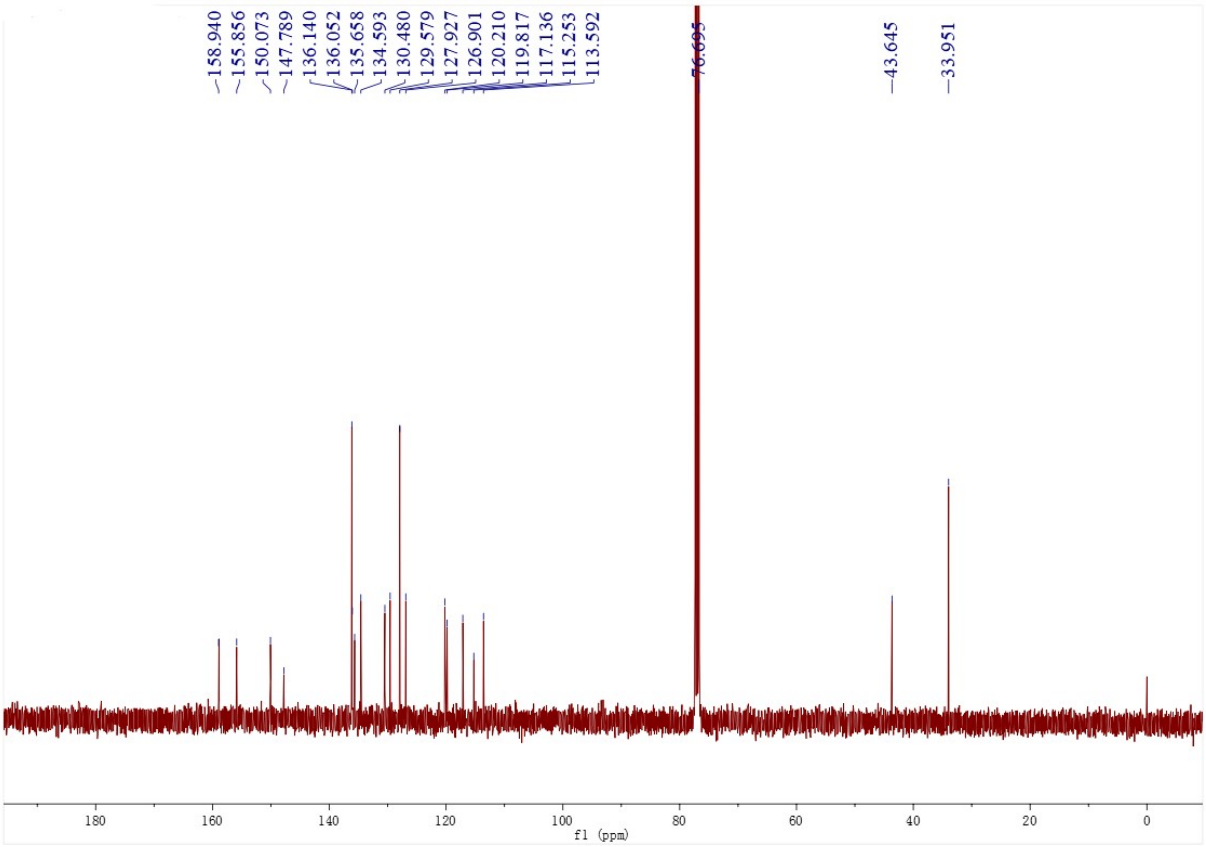

Figure S4. The ^{13}C NMR spectrum of BOC-PSi in $CDCl_3$.

2. Characterization

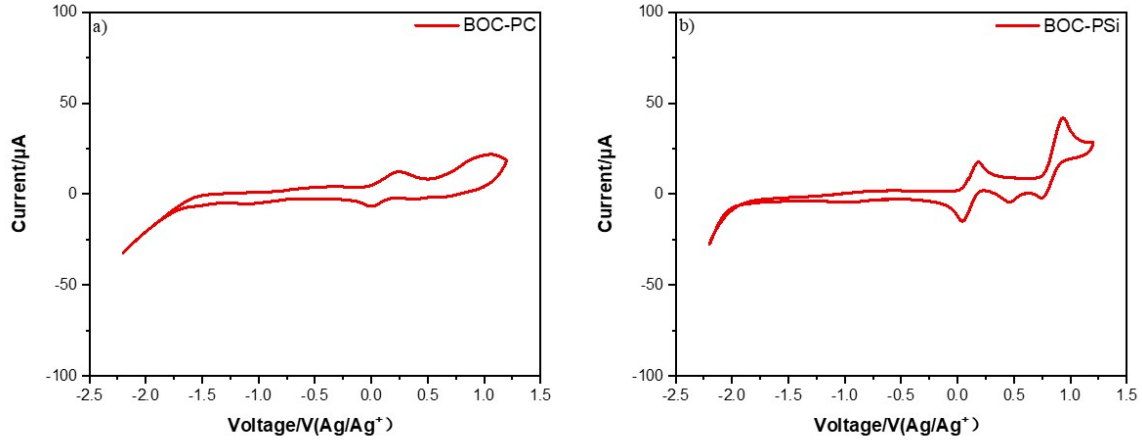

Figure S5. The cyclic voltammograms of compounds a) BOC-PC and b) BOC-PSi in CH_2Cl_2.

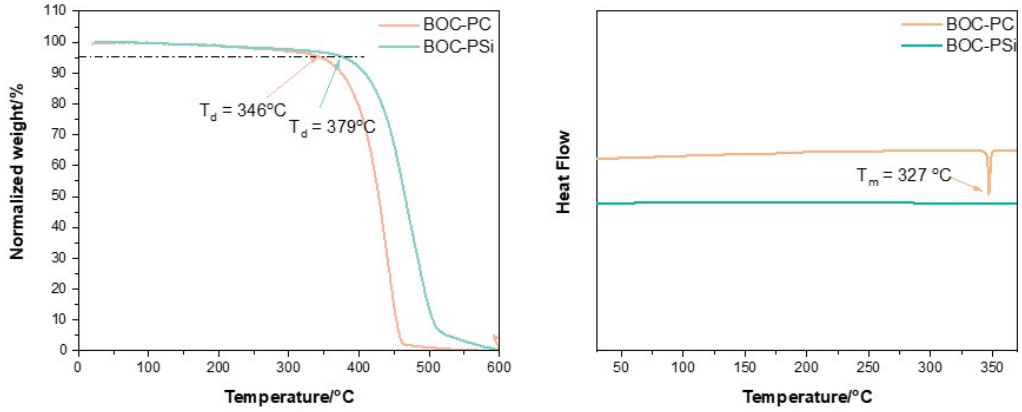

Figure S6. The TGA (left) and DSC (right) thermogram of compounds BOC-PC and BOC-PSi.

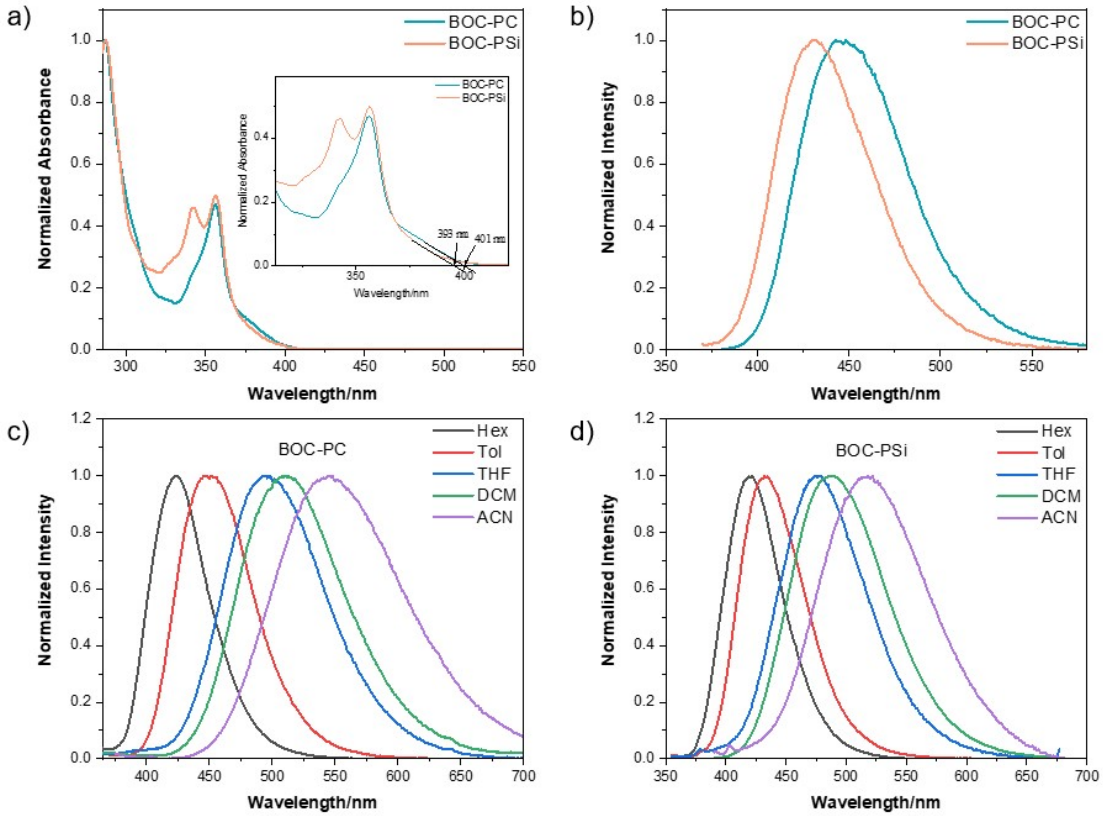

Figure S7. a) The UV-vis absorption and b) PL spectra of BOC-PC and BOC-PSi in toluene (10 μM); the PL spectra of c) BOC-PC and d) BOC-PSi in various solvents (10 μM, λ_{ex}: 340 nm). Hex, *n*-hexane; Tol, toluene; THF, tetrahydrofuran; DCM, dichloromethane; ACN, acetonitrile.

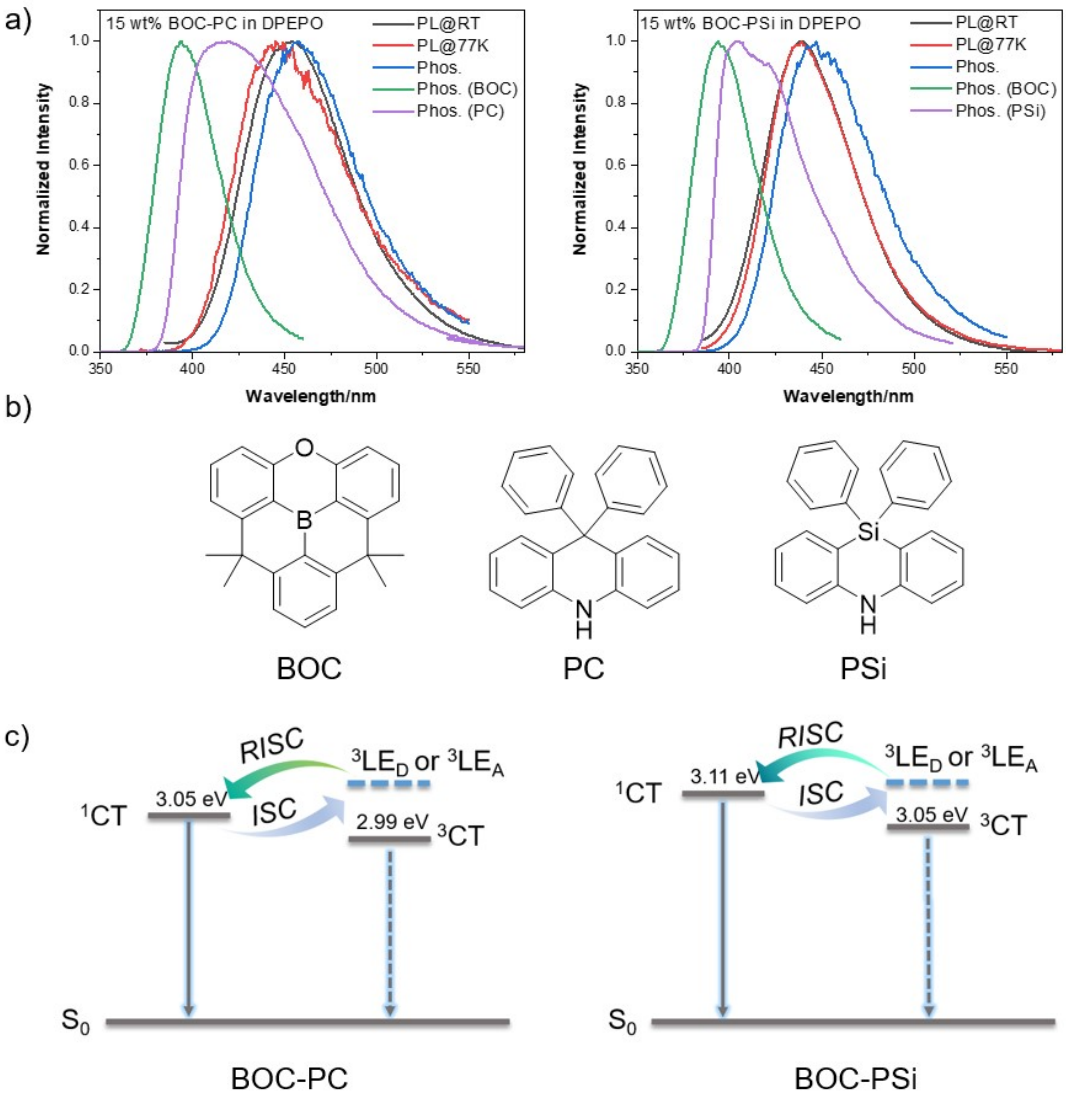

Figure S8. a) The steady-state PL (RT, 77 K), phosphorescence spectra (77 K, delayed 100 ms) of 15 wt% emitters doped DPEPO film and phosphorescence spectra of donor (PC or PSi) and acceptor (BOC) in methylcyclohexane; b) the chemical structure of BOC, PC and PSi; c) the experimental energy alignment of two emitters in DPEPO at 15 wt% doping concentration.

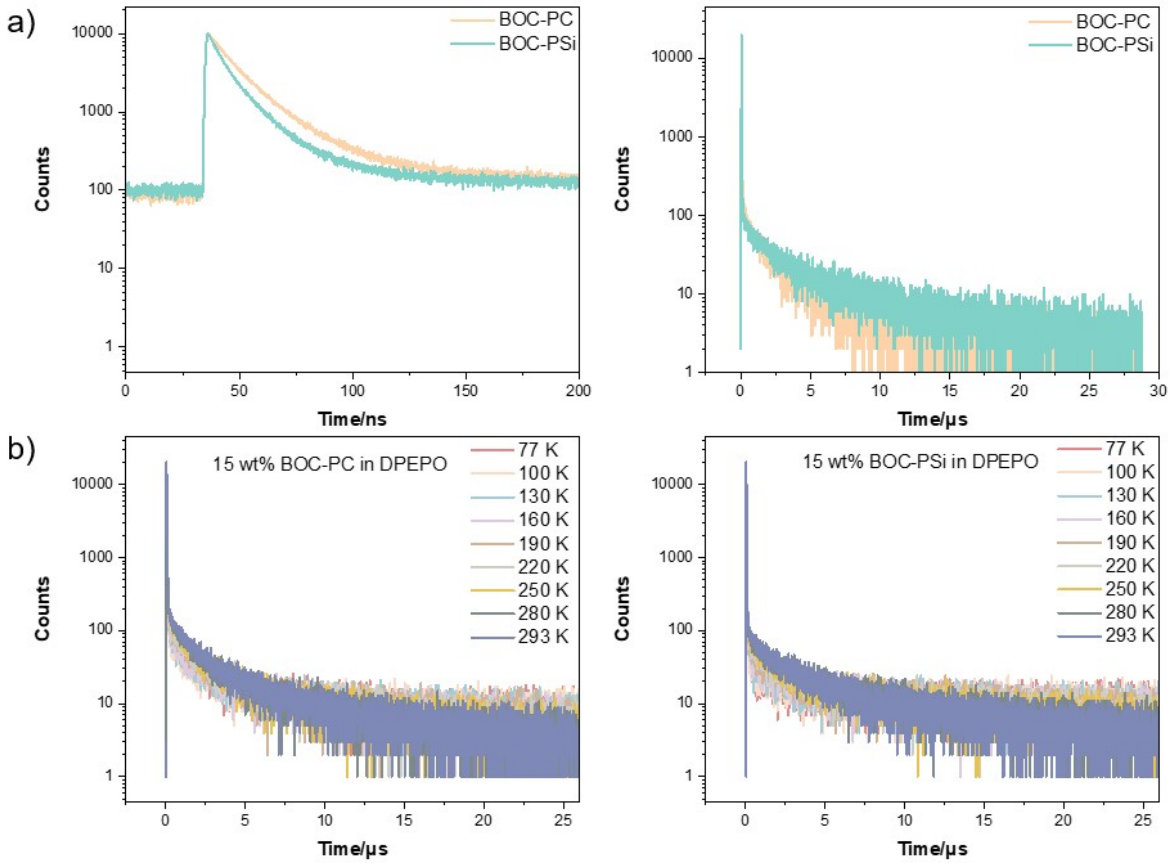

Figure S9. a) The PL decay curves of PF (left) and DF (right) for 15 wt% BOC-PC and BOC-PSi doped DPEPO film under nitrogen; b) temperature-dependent transient PL decay profiles of emitters in doped film under vacuum condition (λ_{ex}: 370 nm, λ_{em}: 440 nm for BOC-PSi and 450 nm for BOC-PC).

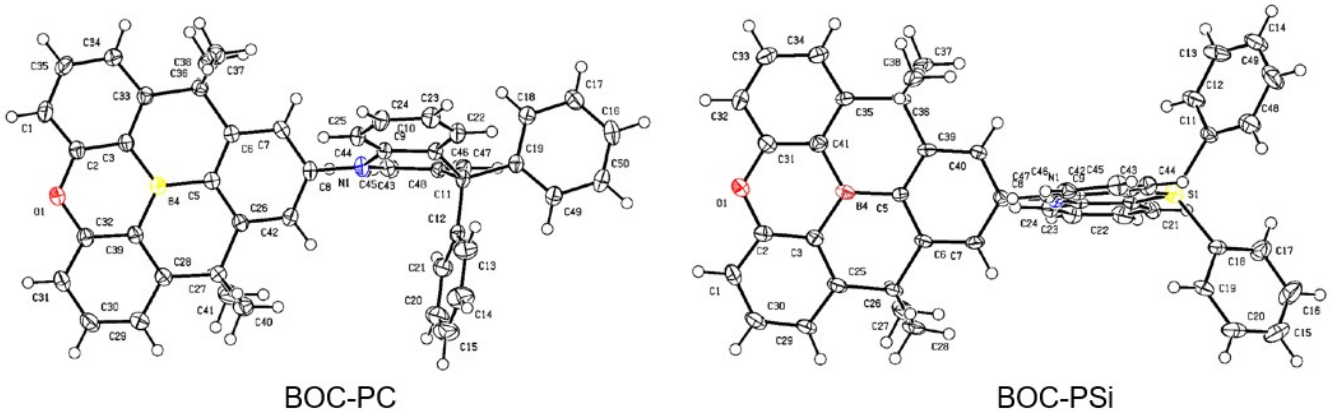

Figure S10. The single crystal structures of a) BOC-PC and b) BOC-PSi.

Table S1. Comparison of crystal experimental data between BOC-PC and BOC-PSi.

	BOC-PC		BOC-PSi	
bond length	N1-C8	1.441 Å	N1-C8	1.448 Å
	B4-C39	1.495 Å	B4-C41	1.493 Å
	B4-C3	1.495 Å	B4-C3	1.494 Å
	B4-C5	1.502 Å	B4-C5	1.497 Å
	C10-C11	1.530 Å	C10-S1	1.848 Å
	C19-C11	1.537 Å	C43-S1	1.852 Å
	C12-C11	1.559 Å	C18-S1	1.880 Å
	C48-C11	1.523 Å	C11-S1	1.882 Å
bond angle	C10-C11-C12	105.94 °	C10-S1-C43	101.35 °
	C10-C11-C48	108.05 °	C10-S1-C18	112.05 °
	C48-C11-C12	108.77 °	C11-S1-C43	112.12 °
	C12-C11-C19	111.90 °	C11-S1-C18	110.19 °
torsion angle	C43-N1-C8-C42	86.38 °	C9-N1-C8-C7	84.02 °
dihedral angle	(C10-C23-C25)-(C46-C44-C48)	24.03 °	(C43-C45-C47)-(C10-C22-C24)	6.07 °

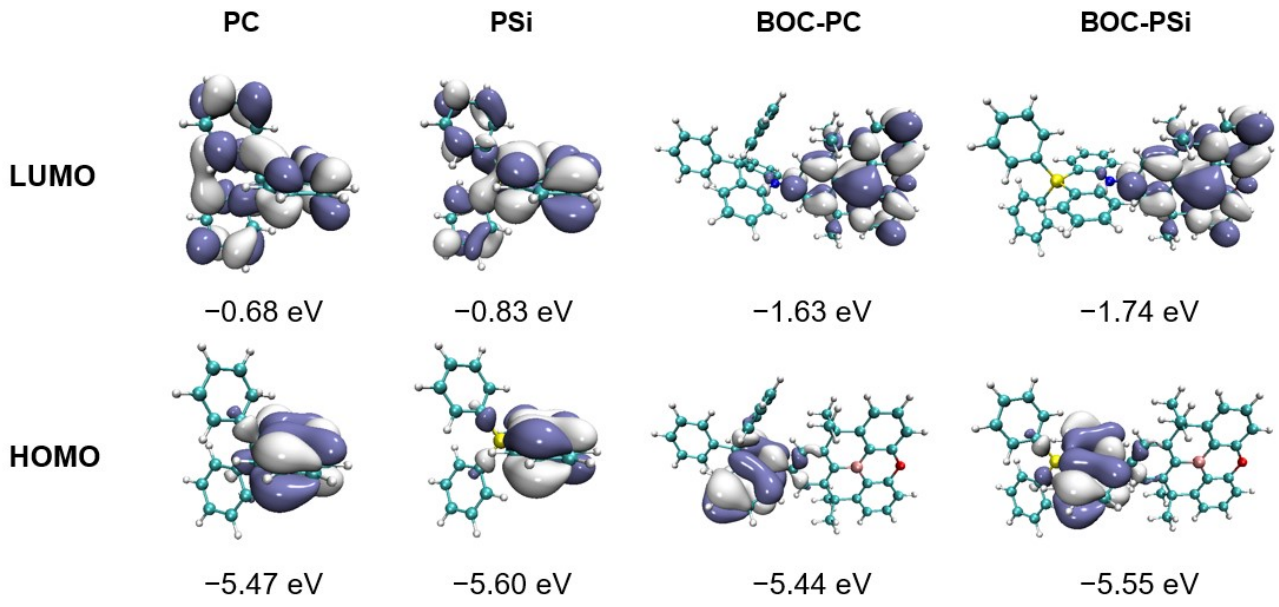

Figure S11. The calculated HOMO/LUMO distribution based on DFT method.

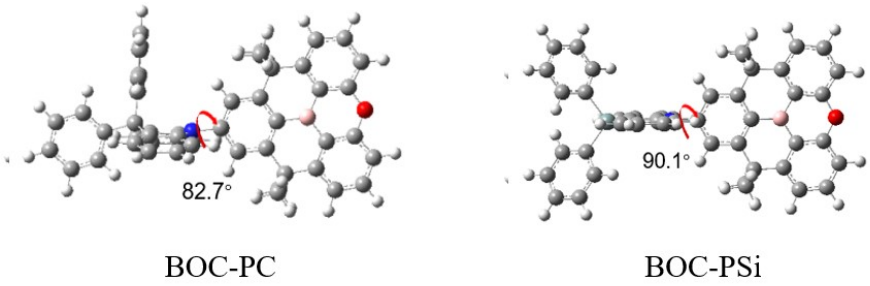

Figure S12. Optimized S_0 geometric structures of BOC-PC and BOC-PSi.

a)

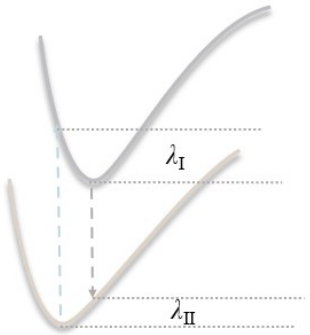

$\lambda = \lambda_I + \lambda_{II}$

	λ_I	λ_{II}	λ
BOC-PC	0.14 eV	0.16 eV	0.30 eV
BOC-PSi	0.11 eV	0.09 eV	0.20 eV

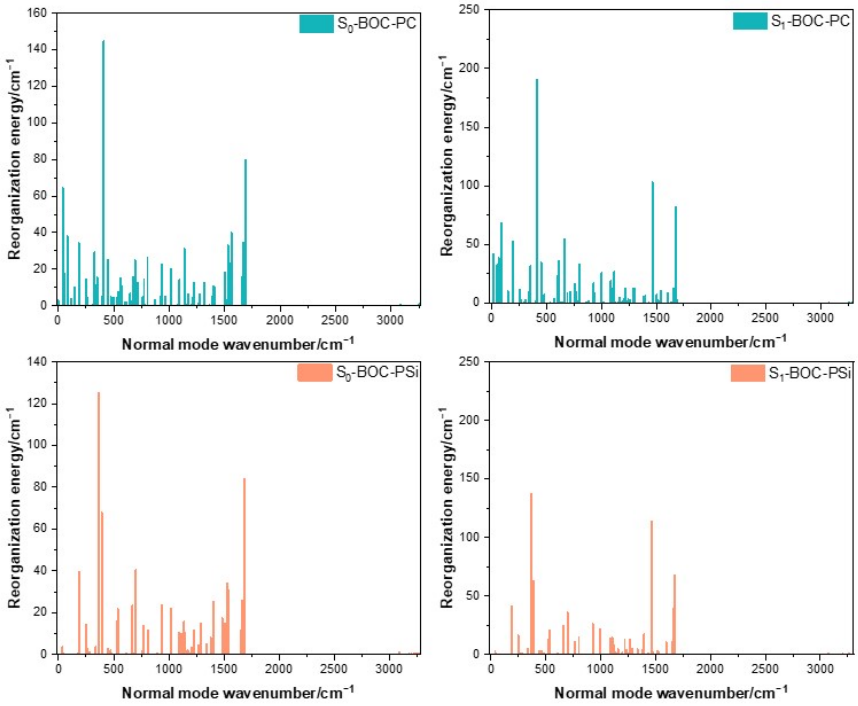

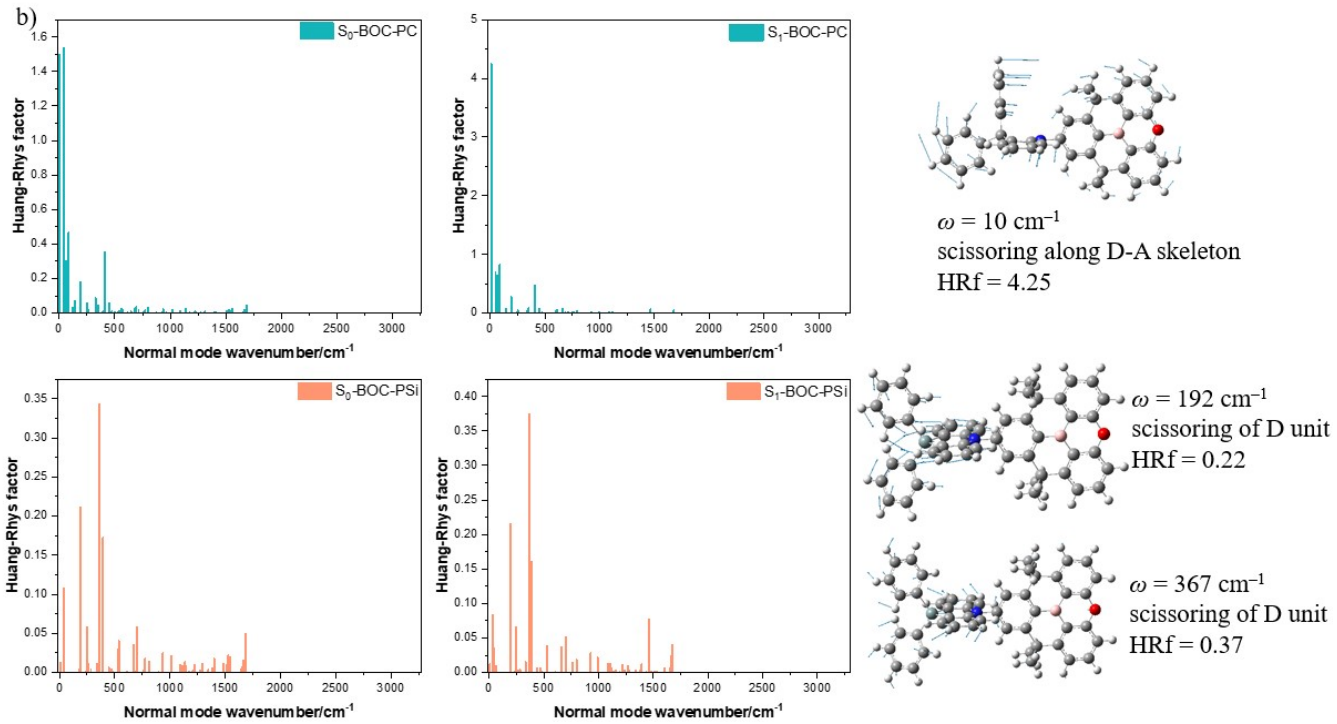

Figure S13. a) The calculated total reorganization energy and decomposed reorganization energy at various normal vibration modes; b) the calculated Huang-Rays factors and vibration mode for BOC-PC and BOC-PSi.

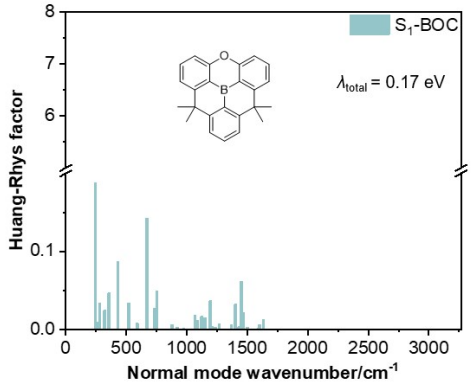

Figure S14. The calculated total reorganization energy and Huang-Rays factors for BOC units.

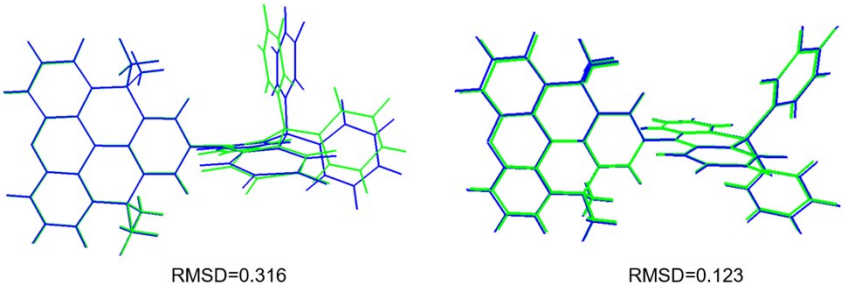

Figure S15. The geometrical difference between the optimized S_0 and S_1 states of BOC-PC and BOC-PSi.

Table S2. Summary of physical properties for two emitters.

Compounds	λ_{em}[a] (nm)	T_d/T_g (°C)	E_{S_1}[b] (eV)	E_{T_1}[c] (eV)	$\Delta E_{S_1T_1}$ (eV)	HOMO (eV)	LUMO (eV)	E_g[g] (eV)
BOC-PC	445	383/327	3.06	2.99	0.07	−5.41[d]/−5.44[f]	−2.32[e]/−1.63[f]	3.09
BOC-PSi	432	379/-	3.11	3.05	0.06	−5.53[d]/−5.55[f]	−2.37[e]/−1.74[f]	3.16

[a] In toluene (10 μM). [b] Calculated from onset of fluorescence spectra in 15 wt% doping film at RT. [c] Calculated from onset of phosphorescence spectra in 15 wt% doping film at 77 K. [d] Experimentally determined from onset of cyclic voltammetry curves in DCM: E_{HOMO} (eV) = − [4.8 + (E_{ox} − $E_{(Fc+/Fc)}$)] eV. [e] Determined from the formular: E_{LUMO} (eV) = E_{HOMO} + E_g. [f] Theoretically calculated in DCM; [g] Experimentally determined from the onset of absorption spectra.

3. The performance of OLED

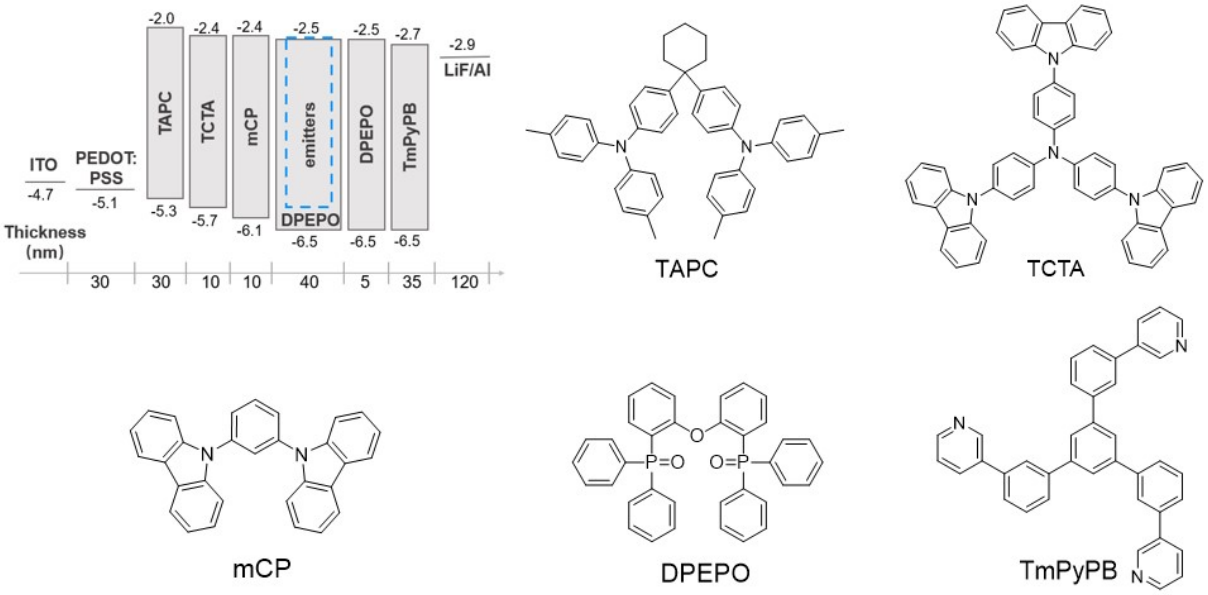

Figure S16. The chemical structure of functional layer materials and OLED structure for device I-II.

Table S3. Summary of EL properties for doped-OLED based on two emitters.

Dopant	Device	V_{on} (V)	λ_{EL} (nm)	FWHM (nm)	CE_{max} (cd·A^{-1})	EQE_{max}/EQE_{100} [%]	Roll-off	CIE_{1931}
BOC-PC	I	3.6	450	62	11.1	14.8/2.8	85%	(0.148,0.085)
BOC-PSi	II	4.4	433	53	9.1	19.6/14.8	24%	(0.154,0.049)

Table S4. Summary of the reported deep-blue ($CIE_y \leq 0.06$) TADF emitters.

Emitter	Emitter type	EML	λ_{EL} (nm)	FWHM (nm)	EQE_{max}/EQE_{100} [%]	CIE_{1931} (x,y)	Reference
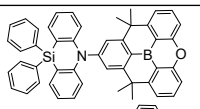	D-A TADF	In DPEPO	433	53	19.6/14.8	(0.154,0.049)	**This work**
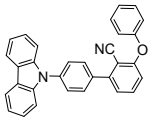	D-A TADF	Nondoped	404	51	5.3/4.8	(0.160,0.034)	[5]
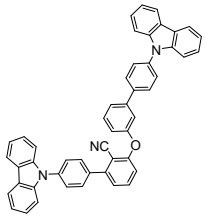	D-A TADF	Nondoped	404	52	7.5/7.4	(0.159,0.035)	[5]
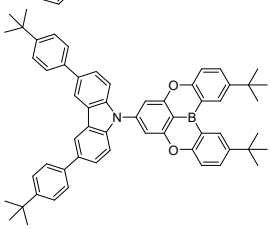	D-A TADF	Nondoped	428	42	15.8/12.0	(0.16, 0.05)	[6]
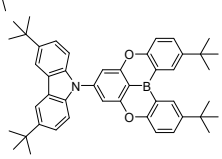	D-A TADF	In mCP	412	44	15.9/12.7	(0.17, 0.06)	[6]
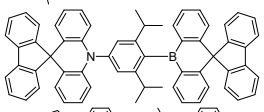	D-A TADF	In DPEPO	440	50	23.4/-	(0.155, 0.047)	[7]
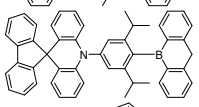	D-A TADF	In DPEPO	430	50	15.4/-	(0.155, 0.047)	[7]
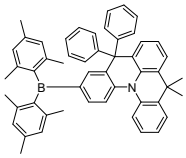	D-A TADF	In DPEPO	444	44	10.0/-	(0.151, 0.045)	[8]
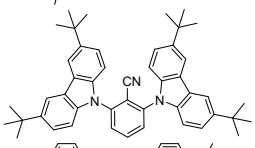	D-A TADF	In DPEPO	428	65	10.3/5.4	(0.16, 0.06)	[9]
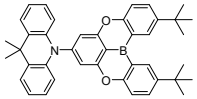	D-A TADF	In PPBI	448	48	21.5/-	(0.15, 0.06)	[10]
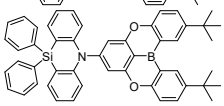	D-A TADF	In DPEPO	436	50	21.6/17.7	(0.154, 0.046)	[11]
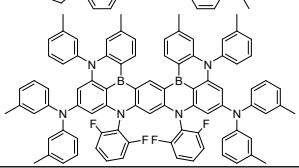	MR-TADF	In DBFPO	461	18	33.7/-	(0.13, 0.06)	[12]

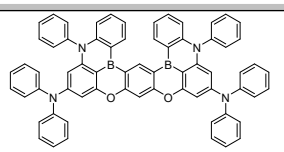	MR-TADF	In mCBP	445	18	13.6/9.8	(0.15, 0.04)	[13]
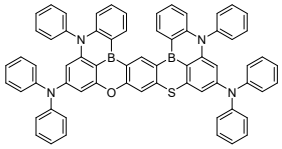	MR-TADF	In mCBP	456	23	26.9/24.0	(0.14, 0.06)	[13]
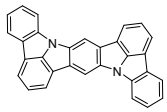	MR-TADF	In mCP:TSPO1	437	24	6.5/-	(0.16, 0.04)	[14]
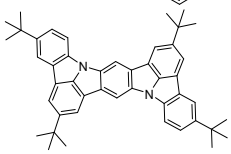	MR-TADF	In mCP:TSPO1	445	22	15.1/-	(0.16, 0.05)	[14]
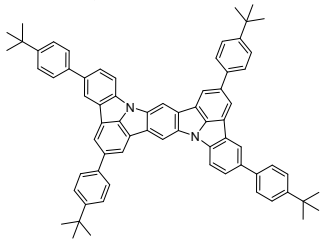	MR-TADF	In mCP:TSPO1	452	21	23.1/	(0.15, 0.05)	[14]
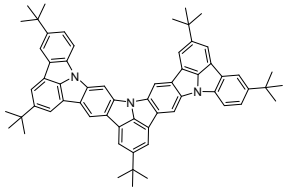	MR-TADF	In mCP:TSPO1	446	21	24.3/4.4	(0.154, 0.044)	[15]
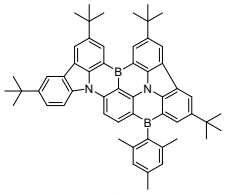	MR-TADF	In mCBP: m4TCzPhBN	452	17	33.9/	(0.144, 0.058)	[16]
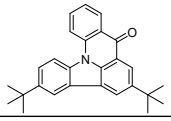	MR-TADF	In mCP	432	35	15.6/6.0	(0.154,0.047)	[17]

4. Parameters of photophysical processes

Assuming that the relative rate constants for the singlet excitons are considerably larger than the triplet excitons, namely $k_r + k_{NR}^S + k_{ISC} >> k_{RISC} + k_{NR}^T$, k_{PF} and k_{DF} was estimated according to the following equations.

$$k_{PF} = \frac{1}{\tau_{PF}} = k_r + k_{ISC} + k_{NR}^S \quad (1)$$

$$k_{DF} = \frac{1}{\tau_{DF}} \quad (2)$$

$$\Phi_{PF} = \frac{k_r}{k_r + k_{ISC} + k_{NR}^{S}} \quad (3)$$

$$\Phi_{DF} = \sum_{n=1}^{\infty} (\Phi_{ISC}\Phi_{RISC})^n \Phi_{PF} = \frac{\Phi_{ISC}\Phi_{RISC}}{1 - \Phi_{ISC}\Phi_{RISC}} \Phi_{PF} \quad (4)$$

In the case that the non-radiative process is significantly slower than RISC process, signifying that $\Phi_{RISC} \approx 1$.

$$k_r = \frac{\Phi_{PF}}{\tau_{PF}} \quad (5)$$

$$k_{ISC} = k_{PF} \frac{\Phi_{DF}}{\Phi_{DF} + \Phi_{PF}} \quad (6)$$

$$k_{RISC} \approx \frac{k_{PF} \cdot k_{DF}}{k_{ISC}} \cdot \frac{\Phi_{DF}}{\Phi_{PF}} \quad (7)$$

$$k_{NR}^{S} = k_{PF} - k_{ISC} - k_r \quad (8)$$

References

[1] J. R. Reimers, *J. Chem. Phys.* **2001**, *115*, 9103-9109.

[2] T. Kushida, C. Camacho, A. Shuto, S. Irle, M. Muramatsu, T. Katayama, S. Ito, Y. Nagasawa, H. Miyasaka, E. Sakuda, N. Kitamura, Z. Zhou, A. Wakamiya, S. Yamaguchi, *Chem. Sci.* **2014**, *5*, 1296-1304.

[3] M. Melaimi, S. Sole, C.-W. Chiu, H. Wang, F. P. Gabbai, *Inorg. Chem.* **2006**, *45*, 8136-8143.

[4] I. S. Park, H. Min, J. U. Kim, T. Yasuda, *Adv. Opt. Mater.* **2021**, *9*, 2101282.

[5] J. Chen, H. Liu, J. Guo, J. Wang, N. Qiu, S. Xiao, J. Chi, D. Yang, D. Ma, Z. Zhao, B. Z. Tang, *Angew. Chem. Int. Ed.* **2022**, *134*, e202116810.

[6] H. J. Kim, H. Kang, J. E. Jeong, S. H. Park, C. W. Koh, C. W. Kim, H. Y. Woo, M. J. Cho, S. Park, D. H. Choi, *Adv. Funct. Mater.* **2021**, *31*, 2102588.

[7] G. Xia, C. Qu, Y. Zhu, J. Ye, K. Ye, Z. Zhang, Y. Wang, *Angew. Chem. Int. Ed.* **2021**, *60*, 9598–9603.

[8] A. Khan, X. Tang, C. Zhong, Q. Wang, S. Y. Yang, F. C. Kong, S. Yuan, A. S. D. Sandanayaka, C. Adachi, Z. Q. Jiang, L. S. Liao, *Adv. Funct. Mater.* **2021**, *31*, 2009488.

[9] C.-Y. Chan, L.-S. Cui, J. U. Kim, H. Nakanotani, C. Adachi, *Adv. Funct. Mater.* **2018**, *28*, 1706023.

[10] D. H. Ahn, S. W. Kim, H. Lee, I. J. Ko, D. Karthik, J. Y. Lee, J. H. Kwon, *Nat. Photonics.* **2019**, *13*, 540-546.

[11] H.-J. Tan, G.-X. Yang, Y.-L. Deng, C. Cao, J.-H. Tan, Z.-L. Zhu, W.-C. Chen, Y. Xiong, J. X. Jian, C.-S. Lee, Q.-X. Tong, *Adv. Mater.* **2022**, *34*, 2200537.

[12] K. R. N, L. Hyuna, B. Ramanaskanda, J. Y. Ki, J. H. Soon, H. K. Jang, *Chem. Eng. J.* **2021**, *432*, 134381.

[13] I. S. Park, M. Yang, H. Shibata, N. Amanokura, T. Yasuda, *Adv. Mater.* **2022**, *34*, 2107951.

[14] V. V. Patil, H. L. Lee, I. Kim, K. H. Lee, W. J. Chung, J. Kim, S. Park, H. Choi, W. J. Son, S. O. Jeon, J. Y. Lee, *Adv. Sci.* **2021**, *8*, 2101137.

[15] J. Kang, S. O. Jeon, H. L. Lee, J. Lim, U. Jo, J. Y. Lee, *Mater. Today.* **2023**, *69*, 88-96.

[16] L. Wang, X. Wang, G. Meng, X. Zeng, D. Zhang, L. Duan, , *Sci. Adv.* **2023**, *9*, eadh143.

[17] C. Cao, J.-H. Tan, Z.-L. Zhu, J.-D. Lin, H.-J. Tan, H. Chen, Y. Yuan, M.-K. Tse, W.-C. Chen, C.-S. Lee, *Angew. Chem. Int. Ed.* **2023**, *62*, e202215226.